MTH9903 Capstone Project

Roughness Over Time: A VIX Futures Perspective

Gabriele Bernardino Niccolò Fabbri

Master in Financial Engineering Program
Baruch College, City University of New York

Supervisor: Professor Jim Gatheral

December 24, 2024

Abstract

This project leverages the pricing formula of Jacquier et al. [2018] to examine how the rough Bergomi model can be calibrated to VIX futures data, with a particular focus on the time evolution of the roughness parameter H. Our findings suggest that H can offer valuable information on periods of market stress, underscoring the relevance of rough volatility modeling in practice.

1 Introduction

Volatility lies at the core of modern finance, playing a crucial role in everything from risk management to derivative pricing. A central insight from recent studies is that volatility often appears to be *rough*, meaning it behaves more like a fractional Brownian motion with a Hurst exponent in $(0, 1/2)$. In light of this, the *rough Bergomi* (rBergomi) model introduces fractional kernels into the classical Bergomi framework, capturing the slowly decaying autocorrelation commonly found in empirical volatility data. In this project, we use the rBergomi model to investigate the pricing of VIX futures, focusing on two main questions: how to calibrate the model in practice, and whether the roughness parameter H can serve as a market indicator.

After laying out the essentials of rough volatility and the VIX in Section 2, we introduce the specific version of the rBergomi model that we use, emphasizing its lognormal approximation for VIX futures. Our attention then turns to the data, described in Section 3, where we use OptionMetrics quotes on VIX options and futures over a long historical period, removing illiquid maturities and carefully cleaning the dataset. We detail how the Carr Madran replication formula can be employed to extract forward variance curves from market prices, and we explain how the calibration problem ultimately reduces to estimating a pair of key parameters: the roughness parameter H and the volatility-of-volatility parameter η. Alongside this market-based estimation, we also implement an autocorrelation-based procedure grounded in daily realized variance of the S&P 500, allowing us to compare two distinct approaches to assessing roughness.

In Section 4, we examine the behavior of H across time, showing how it moves in tandem with major market events particularly those marked by large volatility spikes. Finally, Section 5 discusses how one might convert these insights into trading signals in the VIX futures market, testing both a *buy rough, sell smooth* rule that flips between long and short volatility exposures and a purely *short-volatility* strategy that halts trading under rough conditions. While the first approach performs well in some crises (notably COVID-19) but less so in others, the second strategy generally benefits from a roughness-based stop-trading mechanism, helping to reduce drawdowns.

2 Rough Volatility and VIX

It is a widely accepted fact in the literature that volatility is rough (Gatheral et al. [2018]), i.e., it behaves similarly to a fractional Brownian Motion (fBM) with Hurst exponent $H \in (0, 1/2)$. More precisely, as in Bayer et al. [2015], we model volatility as a fractional Ornstein-Uhlenbeck process:

$$\begin{aligned} \frac{dS_t}{S_t} &= \sqrt{V_t} dZ_t \\ d(\log V_t) &= -\alpha(\log V_t - \theta)dt + \nu dW_t^H \end{aligned} \tag{2.1}$$

where W_t^H is a fBM which is allowed to be correlated with Z_t and α, $\nu > 0$ and $\theta \in \mathbb{R}$ are parameters describing the mean-reversion of log-volatility.

Volatility models are often specified via the forward variance curve, defined as:

$$\xi_t(u) := \mathbb{E}[V_u | \mathcal{F}_t], \quad u \geq t.$$

2.1 The Rough Bergomi Model

The model used in this paper starts from the so-called n-factor Bergomi model (Bergomi [2005]):

$$\xi_t(u) = \xi_0(u)\mathcal{E}\left(\sum_{i=0}^{n} \eta_i \int_0^t e^{-\kappa_i(u-s)} dW_s^{(i)}\right), \tag{2.2}$$

where $\mathcal{E}(\cdot)$ is the stochastic (Wick) exponential. Note that the Bergomi model in this version does not account for the roughness of volatility. Also, this model has two main drawbacks:

1. It is overparametrized: to achieve a decent fit, one would need at least two factors, leading to 8 parameters (plus the initial variance curve $\xi_0(u)$);
2. It generates an exponentially decaying term-structure of the ATM vol skew $\psi(T) := \left|\frac{\partial}{\partial k}\sigma_{BS}(k,T)\right|_{k=0}$, which contrasts with the (often) observed power-law decay.

Those problems can be addressed by combining this model with the insights from rough volatility by replacing the exponential kernels with a single power law of the form $\int_0^t \frac{dW_s}{(u-s)^\gamma}$, $\gamma := 1/2 - H$, which is known as a "Volterra" fBM. This leads to the following specification for the instantaneous variance process:

$$\begin{aligned} V_t &= \xi_0(t)\mathcal{E}\left(\eta \int_0^t \frac{dW_s^{\mathbb{P}}}{(u-s)^\gamma}\right) \\ &= \xi_0(t)\mathcal{E}\left(2\nu C_H \mathcal{V}_t\right) \end{aligned} \tag{2.3}$$

which matches the definition in Jacquier et al. [2018] with $C_H = \sqrt{\frac{2H\Gamma(2-H_+)}{\Gamma(H_+)\Gamma(2-2H)}}$ and $\mathcal{V}_t = \int_0^t (t-u)^{H_-} dZ_u$ (using the notation $H_\pm := H \pm \frac{1}{2}$). We can see from (2.3) that the vol-of-vol parameter can be specified as either η or ν, with the relationship given by $\eta = 2\nu C_H \sqrt{2H}$.

This version of the Bergomi model can now generate smiles and skews that are consistent with empirical observations in equity options, as well as incorporate the known rough properties of volatility. However, since the processes above are described under the physical probability measure $\mathbb{P}$, a change of measure from $\mathbb{P}$ to $\mathbb{Q}$ is needed to fully describe the 'rough Bergomi' (rBergomi for short) model:

$$dW_s^{\mathbb{P}} = dW_s^{\mathbb{Q}} + \lambda_s ds \tag{2.4}$$

Bayer et al. [2015] decide to use a deterministic function $\lambda(s)$ for the change of measure; while this has the drawback of generating flat VIX option smiles (inconsistent with reality, as shown below in Section 3.1), it makes the model simpler and allows for good calibration results.

2.2 The VIX

This project focuses on VIX futures contracts in the framework of the rough Bergomi model. A VIX futures with maturity T is determined by its terminal value, which we call $\sqrt{\zeta(T)}$; it will be convenient to work in terms of the square of this quantity:

$$\zeta(T) := \frac{1}{\Delta} \int_T^{T+\Delta} \mathbb{E}[V_u | \mathcal{F}_T] du, \tag{2.5}$$

where Δ is fixed at one month for all contracts. In other words, the payoff represents the expectation of the average total variance in the month following the expiration of the contract.

2.3 Log-normal distirbution of VIX futures

It is common to model variance as log-normally distributed, consistently with empirical observations; this is also the case for the specification of the instantaneous variance V_t in the rough Bergomi model described above. As in Bayer et al. [2015], we extend this assumption to also hold for $\zeta(T)$ and $\sqrt{\zeta(T)}$; previous research (see Dufresne [2004]) has shown that the integral of a log-normal asymptotically tends to log-normal under certain conditions. Under this approximation, the VIX futures distribution is entirely defined by its first two moments.

The conditional expectation of $\zeta(T)$ at the current time t is easily obtained using

tower property:

$$\begin{aligned}\mathbb{E}[\zeta(T)|\mathcal{F}_t] &= \frac{1}{\Delta}\int_T^{T+\Delta} \mathbb{E}\left[\mathbb{E}[V_u|\mathcal{F}_T]|\mathcal{F}_t\right] = \frac{1}{\Delta}\int_T^{T+\Delta} \mathbb{E}[V_u|\mathcal{F}_t]du = \\ &= \frac{1}{\Delta}\int_T^{T+\Delta} \xi_t(u)du\end{aligned} \tag{2.6}$$

Regarding the second moment of the distribution, Jacquier et al. [2018] derive an exact yet lengthy formula requiring no further assumption. However, their formula is quite demanding from a computational point of view and thus does not lend itself too well to the calibration task we are concerned with. On the other hand, Bayer et al. [2015] show how to derive a much simpler expression for $\mathrm{Var}[\log\zeta(T)|\mathcal{F}_t]$ by approximating the arithmetic mean of ζ with the geometric mean. Note that Jacquier et al. [2018] themselves show that this approximation is actually very accurate. The resulting formula is:

$$\mathrm{Var}[\log\zeta(T)|\mathcal{F}_t] \approx \eta^2(T-t)^2 f_H\left(\frac{\Delta}{T-t}\right), \tag{2.7}$$

where

$$f_H(\theta) := \frac{2H}{H_+^2}\frac{1}{\theta^2}\int_0^1 \left[(1+\theta-x)_+^H - (1-x)_+^H\right]^2 dx \tag{2.8}$$

We can now apply the above results to obtain the fair value of a VIX futures contract by computing the convexity adjustment for the expectation of $\sqrt{\zeta(T)}$:

$$\mathbb{E}[\sqrt{\zeta(T)}|\mathcal{F}_t] = \sqrt{\mathbb{E}[\zeta(T)|\mathcal{F}_t]}\exp\left(-\frac{1}{8}\mathrm{Var}[\log\zeta(T)|\mathcal{F}_t]\right) \tag{2.9}$$

This is the expression for the fair value that we will use for our model and trading strategy.

3 Data and Model Calibration

3.1 The Dataset

3.1.1 VIX Options and Futures

Our dataset comes from OptionMetrics and contains bid and ask quotes for a grid of VIX options, as well as forward prices for the listed maturities, on each trading day from February 24, 2006 to August 31, 2023. In order to obtain reliable fits, we

remove the maturities that have less than 5 listed strikes, as well as the days with less than 5 quoted expiries. This filter only removes 45 days, all of which were in the first year of the sample.

We plot the VIX smiles with raw SVI (Gatheral and Jacquier [2014]) fits in Figure (1) for a representative day. As previously mentioned, VIX smiles tend to exhibit a (positive) skew for all maturities, which the rough Bergomi model cannot capture. Therefore, we expect some margin of error in the estimation of the parameters.

The VIX Futures term structure instead can have a variety of shapes in the observed data, although it is for the most part increasing in time to expiration. Plots of the term structures for representative days are postponed to include model fits as well.

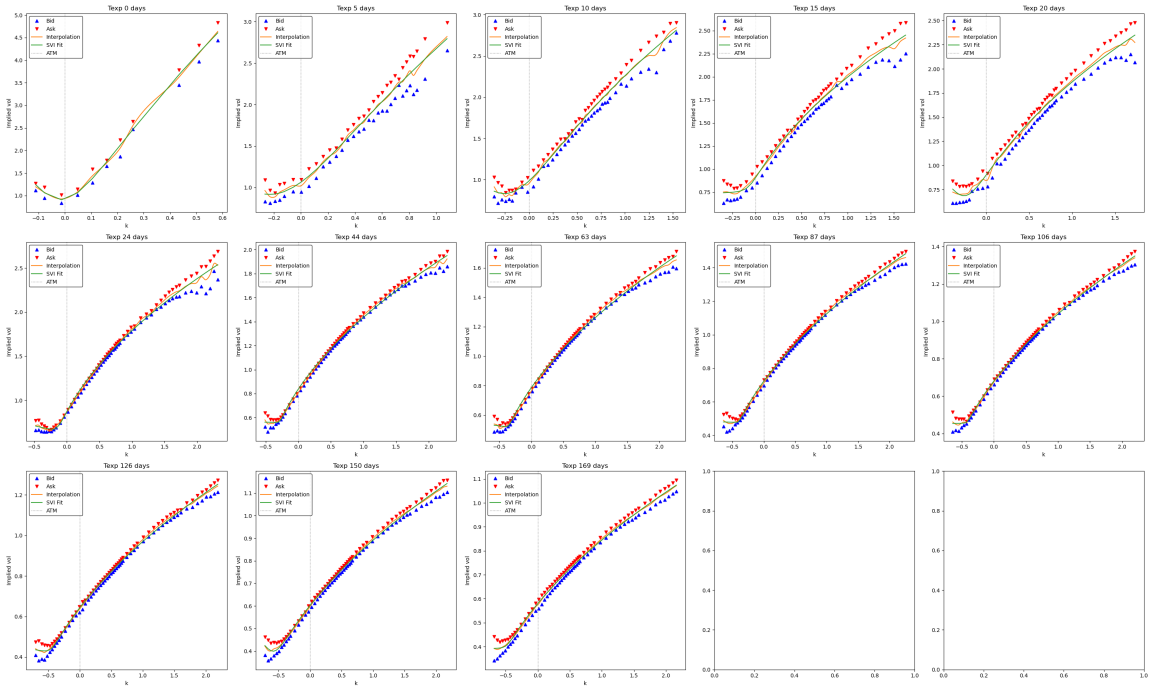

Figure 1: VIX Options smiles on a representative day (2023-08-15)
As it is well known in the literature, VIX smiles have a positive skew at all maturities. The plots include bid (blue triangles) and ask (red triangles) implied volatilities, as well as a Stineman interpolation through the mids (orange line) and a raw SVI fit (green line).

3.1.2 Realized Variance

Since we are particularly interested in the time series behavior of the roughness parameter H and its comovement with market risk and illiquidity, we also studied another estimator based on the autocorrelation function (ACF) of realized variance to see how it relates to the VIX futures-based one. This estimator is based on the

Rendleman-Bartter realized variance estimate, which can be computed directly from the daily low and high prices of SPX. We get those prices from YahooFinance via the python API `yfinance`.

The Rendleman-Bartter estimator is defined as:

$$RV_t = \log\left(\frac{S_t^{high}}{S_t^{low}}\right), \tag{3.1}$$

where t is a daily index and S^{high} and S^{low} indicate the highest and lowest intraday prices of SPX, respectively. The behavior of this estimator is shown in Figure (2). We can observe peaks in the time series around periods of uncertainty and turmoil, as well as the aforementioned approximate log-normality of volatility and variance.

3.2 Calibration to VIX Futures term structure

The bulk of our research lied in the calibration of the approximated lognormal model to the term structure of VIX futures. From (2.7) and (2.9), we see that the output of the model is only a function of $\xi_t(u)$, H and η. The forward variance curve can be estimated in a model-independent way via the Carr-Madran (Carr and Madran [1998]) replication formula, while H and η are the decision variables used in the calibration problem.

The Carr-Madran replication formula can be applied directly to the VIX option prices in our dataset. Since VIX options have payoff $\left(\sqrt{\zeta(T)} - K\right)^+$, we let $Y_T^2 := \zeta(T)$ for a fixed maturity T, so that we can write the payoff function to be replicated as $g(x) = x^2$. Since $g''(x) \equiv 2$, the formula reads:

$$\int_T^{T+\Delta} \mathbb{E}[V_u|\mathcal{F}_t]du = F_{VIX}^2 + 2\int_0^F P(K)dK + 2\int_F^\infty C(K)dK. \tag{3.2}$$

and we obtain $\mathbb{E}[\zeta(T)|\mathcal{F}_t] = \frac{1}{\Delta}\int_T^{T+\Delta} \mathbb{E}[V_u|\mathcal{F}_t]du$. To perform the integration in practice, we use a log-moneyness grid $k \in [-10, 10]$ (where $k := \log(K/S)$), using Stineman interpolation inside the listed strikes and flat extrapolation outside. We also experimented with using SVI for extrapolation and it did seem to marginally improve fits, although not enough to justify the added computational costs.

Regarding the actual estimation of the model parameters, we simply minimize the squared loss between the observed VIX futures prices and the fair value from (2.9). It is interesting to note that classical optimization algorithms (mainly 'L-BFGS-B' in the `scipy.optimize` implementation) would sometimes face identifiability issues whenever it would be possible to achieve a small loss with extremely low values of H and high values of η. To mitigate this, we performed the estimation using a differential evolution algorithm instead, which achieved basically the same loss on problematic dates while finding reasonable parameter values. Table (1) presents a summary of the estimated parameters over time.

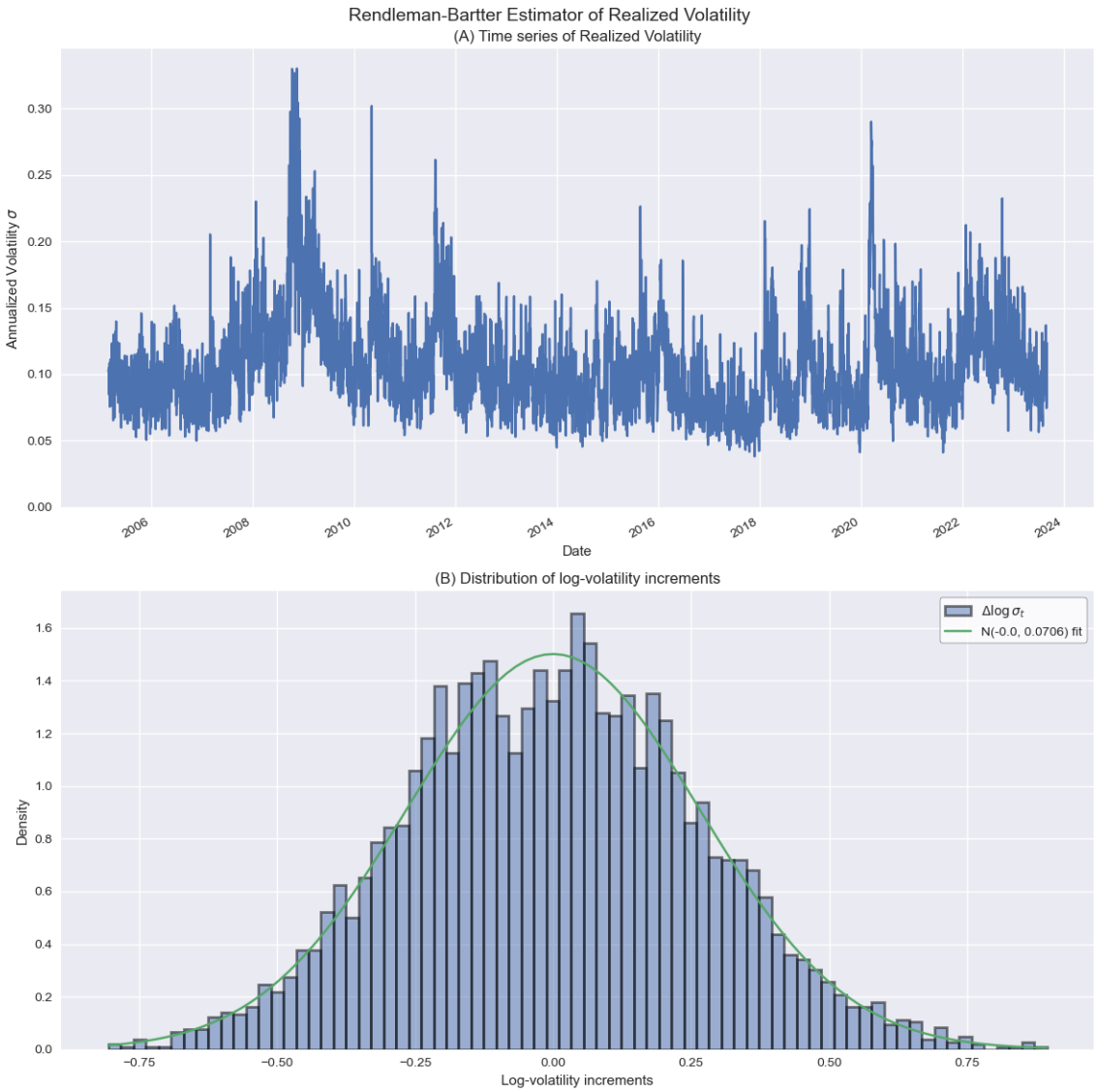

Figure 2: Rendleman-Bartter estimator of realized variance
The estimator is defined in (3.1). Panel (A) shows the time-series behavior of estimated realized variance over the course of our sample; Panel (B) shows the distribution of $\log \sigma_{t+1} - \log \sigma_t$, along with a normal fit.

3.3 ACF-based estimator

To compute an alternative estimation of H, we adapt the method presented in Bennedsen et al. [2016] to apply it to our daily estimate of realized variance, as opposed to their intraday dataset.

	H	η
count	4366	4366
mean	0.079971	6.507569
std	0.077501	11.217024
min	0.000002	0.920649
25%	0.008938	1.498485
50%	0.062901	1.977299
75%	0.134494	4.442452
max	0.500000	100.000000

Table 1: Summary of estimated parameters
Parameters are calibrated according to the procedure explained in Section 3.2. Note that H has been clipped to $[0, 0.5]$, which has affected only 3 values (0.07% of the sample), while η has been clipped to $[0, 100]$.

Formally, let $\rho(\Delta)$ define the autocorrelation function of log-volatility,

$$\rho(\Delta) := \text{Corr}(\log \sigma_{t+\Delta}, \log \sigma_t). \tag{3.3}$$

Then, for a covariance-stationary process that behaves asymptotically as a fBM, the following relation holds:

$$1 - \rho(\Delta) = a\Delta^{2H} \tag{3.4}$$

for some constant a. Therefore, the coefficient from the log-log regression of the rhs on the lhs of (3.4) will give an estimate of $2H$.

To implement the estimator in practice, on each day we estimate the ACF over the past 252 trading days (1 year) for a fixed number of lags (set to 15 based on exploratory analysis) and run the regression (3.4).

3.3.1 ACF and roughness

During the study of this ACF estimator, we observed interesting patterns in the data, which confirmed findings from previous research even for our sample and our very noisy realized variance estimator.

It is considered as a stylized fact of financial markets that volatility clusters over time and tends to be autocorrelated. This originally led to the conclusion that volatility is a long memory process, as opposed to rough. This is because the slowly decaying ACF is often associated with long memory and one way to estimate the Hurst exponent H of a process is from the exponent of the power-law decay of autocorrelation. At first sight, the autocorrelation of realized variance does look like some sort of power law, and applying this method to estimate H does indeed yield estimates above $1/2$, indicating long memory. However, as shown in detail in Gatheral et al. [2018], the

decay of the autocorrelation is only approximately power law and estimating H from (3.4) gives a much better fit.

We briefly explored this debate in our research by looking at the ACF of our realized variance over the entire sample (in addition to the rolling window setting described above). This subsection confirms the rough volatility conclusion in the scope of our project, by showing the empirical ACF of the Rendleman-Bartter estimator (3.1) and comparing the fit of a power law ($H = 0.5568 \in (0.5, 1)$) versus the rough autocorrelation (3.3) ($H = 0.1098 \in (0, 0.5)$). The autocorrelation is plotted on a log-log scale in Figure (3). Note that the points are somewhat close but definitely not on a straight line, and we indeed had to remove the first 20 lags to fit the tail of the power law; on the other hand, the rough autocorrelation fits our data extremely well.

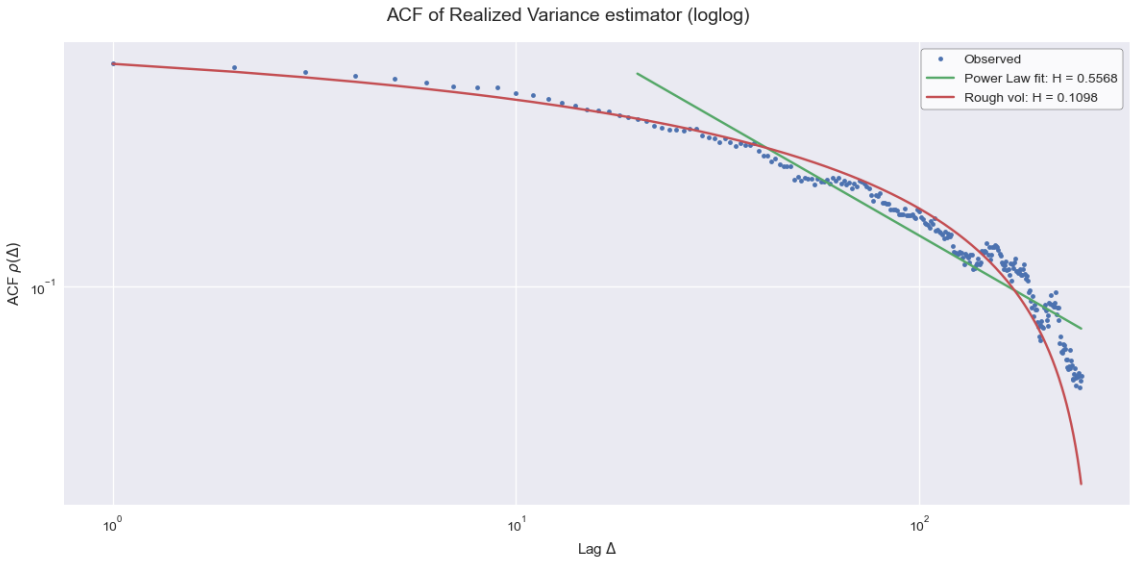

Figure 3: Loglog plot of realized variance ACF
Autocorrelation function of Realized Variance (blue dots), with power law fit (green line) and rough vol fit (red line). Note that the first 20 lags were excluded from the power law fit to focus on the tail.

4 The roughness parameter H

4.1 H as indicator of market conditions

In this paper, we are interested in the practical meaning of the parameter H. Based on previous research, we have some priors about how H relates to market conditions and we intend to compare them with our estimates of the parameter; moreover, the

priors suggest some simple trading rules which we aim to backtest (see Section 5) in order to further validate the analysis.

The time series of the estimator shown in Figure 5 of Bennedsen et al. [2016] shows that the peaks in H more or less align with some known periods of market turmoil (e.g., Lehman bankruptcy). The pattern can also be found in our ACF-based estimator, especially for the biggest events in our sample (Lehman, Covid and Russia invasion of Ukraine). This suggests that H could be taken as an indicator of incoming uncertainty and used for example as a gauge for when to close risky positions.

We also considered some theoretical justifications for this interpretation, although we leave more detailed developments of these ideas for future research. First of all, note that the closer H is to 0.5, the more similarly the process behaves to a standard Brownian motion, thus becoming more and more unpredictable; therefore, it makes sense that H would climb towards this threshold as the market is becoming more and more uncertain. Furthermore, the high-H periods are usually characterized not only by higher risk, but also by lower liquidity; this suggests a connection with the model of El Euch and Rosenbaum [2019], who show that the rough Heston model can be derived as the limit of a Hawkes process-based model of order flow.

By defining a very simple model for the interaction of buy and sell orders which encodes the most well-known stylized facts of high-frequency financial data, they show how the kernel defining the self-excitement of orders within the Hawkes process defines the shape of the kernel of the forward variance curve in a stochastic volatility model. Specifically, El Euch and Rosenbaum [2019] use a power-law decaying self-excitement of order flow, consistent with well-known empirical properties of financial markets, which leads to an extension of the classical Heston model (Heston [2015]), where the kernel of the forward variance curve is again a power law with decay parameter $\alpha - 1$, where $\alpha = H - \frac{1}{2}$. Our idea is that periods of low liquidity can be characterized by slower decay of the order flow impact, meaning a a higher than usual H; on the other hand in a liquid market, an order in a given direction will quickly be absorbed and the convergence to a new steady state will happen sooner, consistent with a faster autocorrelation decay.

4.2 Time series of estimated H

Figure (4) shows the evolution over our dataset of the two estimators of H. What immediately stands out is, as expected, the alignment between the behavior of H and periods of market uncertainty. However, it is interesting to note that the two estimators have slightly different behaviors in this regard.

The rBergomi estimator in Panel (A) seems to spike *after* market events, whereas the ACF estimator in Panel (B) jumps concurrently with those events. If we consider the idea behind the two estimators, this can offer insights into the relationship between H and market conditions. The ACF-based estimator is derived from a proxy for

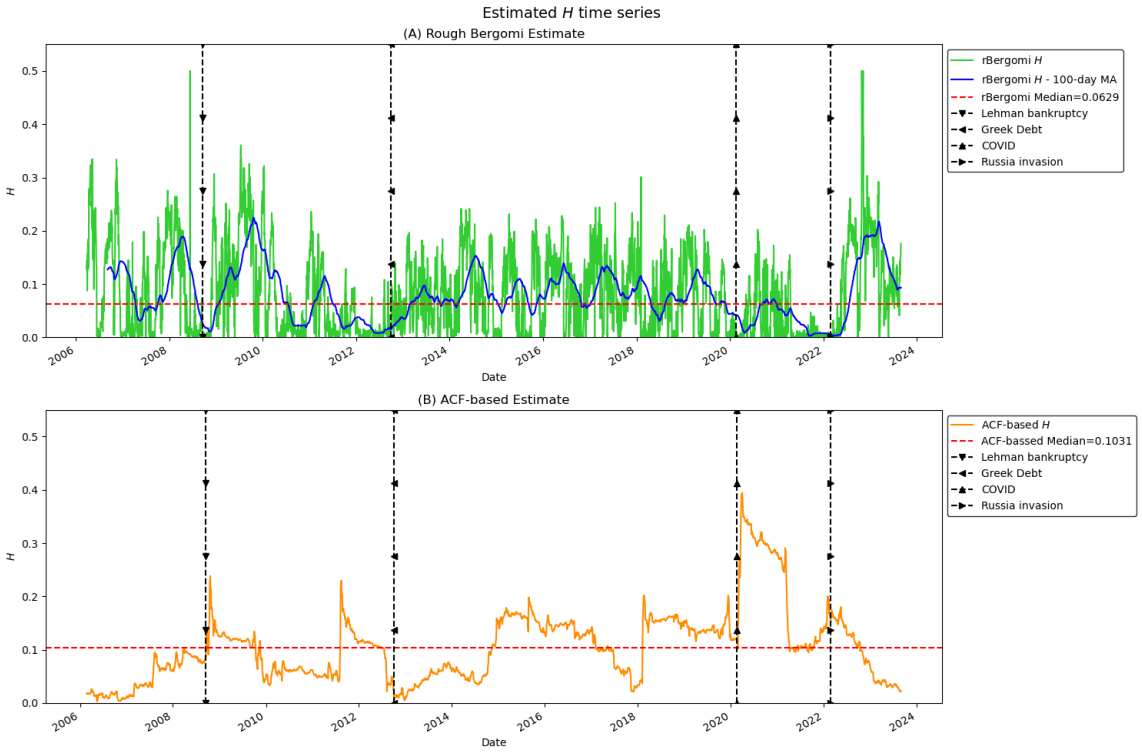

Figure 4: Time series of H estimators
Panel (A) shows the time series of H estimated by fitting the rough Bergomi model to the VIX Futures term structure as explained in Section 3.2. The green line is the bare estimate, while the blue line is smoothed with a 100-day moving average.
Panel (B) plots the ACF-based estimate of H from equation (3.4).
Both panels highlight with the black dashed lines the periods of high market turmoil during the sample.

the true variance process, so one can expect it to respond contemporaneously to underlying market risk. Moreover, the alignment of H with periods of heightened risk further supports the idea that a rough process effectively captures volatility dynamics. Specifically, if volatility is rough then equation (3.4) for its autocorrelation holds, and the estimated H accurately reflects the actual behavior of volatility; its alignment with periods of increased uncertainty is thus consistent with our hypothesis in Section 4.1.

On the other hand, the rBergomi estimator is based on observed market prices of VIX futures, thus reflecting how market participants react to extreme events. In this case, the fact that cycles are aligned with periods of market uncertainty suggests that the rough Bergomi model can effectively capture the pricing methods used by VIX futures market participants.

To assess the goodness of the model and our estimated parameters in describing VIX futures, we plot in Figure (5) some term structures and the calibrated curve

on a number of representative days. The plot shows that futures prices are mostly increasing in time to expiration, although some days display very unusual shapes. Nonetheless, the rBergomi fit can produce very realistic shapes that closely match observed market prices (save for the most extreme term structure curves, such as 2016-01-04). As explained in Section 2.1, we know that this model is a simplification which already does not capture the VIX options skew; therefore, it can be expected that it will not perfectly match other market quantities either, especially under unusual conditions. Still, we can be satisfied with the curves produced by our calibration for our purposes.

Moreover, these plots confirm the idea mentioned in the previous paragraph: the rough version of the Bergomi model seems to capture how traders are pricing VIX futures and volatility in general, which is again strong evidence in favor of the rough volatility hypothesis. While this is a positive conclusion from a theoretical point of view, we believe it is going to make it harder to use this model to implement a trading strategy directly on VIX futures to take advantage of mispricings.

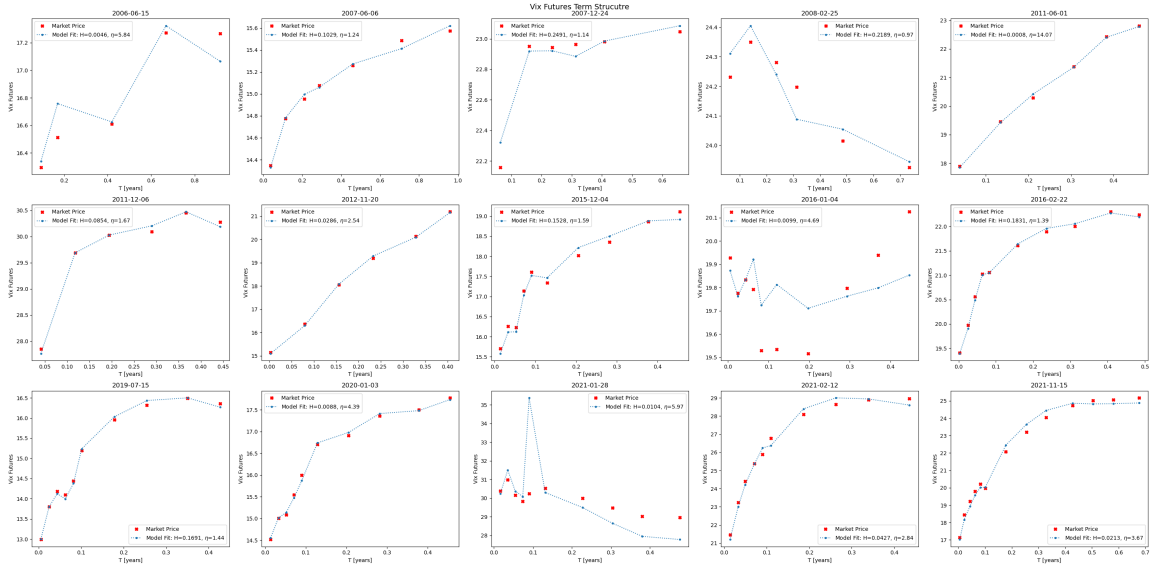

Figure 5: VIX Futures Term Structures and Model Fits
This figure shows the observed term structures of VIX futures prices (red crosses) on a randomly selected subset of the dates, along with the fits from the calibrated rough Bergomi model (blue lines). Parameters estimates H and η are also reported in the legends.
The term structures have pretty regular shapes on most days and the model can fit them very well, although it can happen that the curve will show very strange patterns which are not fully captured.

5 Trading strategy

As stated before, the parameter H, known as the roughness parameter, quantifies the level of roughness in volatility. In rough volatility models, $H < 0.5$ characterizes non-Markovian and rough behavior, which is a defining feature of most financial markets.

Our estimates show that H consistently remains below 0.5, indicating persistent roughness throughout the observed period. To evaluate whether this behavior presents an alpha-generating opportunity, we will test a simple trading strategy: we adopt a "buy rough, sell smooth" approach, loosely inspired by Glasserman and He [2020], using the VIX futures ETF *VXX*. This ETF offers exposure to short-term VIX futures by maintaining positions in the nearest maturity contracts, closely tracking the spot (non-tradable) VIX. This structure ensures that the strategy remains directly linked to volatility dynamics.

The trading strategy is constructed using the rolling mean of the roughness parameter H and its relative position to its rolling median. At time t, the rolling median is denoted as μ_t.

The trading position, π_t, is determined based on the relationship between the estimated roughness parameter H_t and the median:

$$\pi_t = \begin{cases} -1, & \text{if } H_t > \mu_t, \\ 1, & \text{if } H_t < \mu_t, \end{cases}$$

Here:

- $\pi_t = -1$: Represents a **short** position when H_t indicates a smoother volatility regime (above the upper threshold).
- $\pi_t = 1$: Represents a **long** position when H_t indicates a rougher volatility regime (below the lower threshold).

This approach's rationale lies in the nature of the roughness parameter H and in its cyclical, somewhat mean-reverting behavior. When H exceeds the upper threshold, we expect it to soon revert to the usual, rougher levels, indicating a return to typical market conditions and a potential opportunity to short volatility. Conversely, when H falls below the lower threshold, it is usually followed by a spike in consequence of some disruptive event. The expecation of this incoming market stress is a potential opportunity buy volatility.

By dynamically adjusting the thresholds based on rolling statistics, the signal adapts to recent market conditions, ensuring that it remains robust across different volatility regimes. This construction aligns with the mean-reverting behavior of H, capturing deviations from its central tendency.

We can find the Cumulative P&L of the strategy in Figure (6), the background colors (red/green) indicate when the strategy is short or long. With this approach, the strategy successfully captures the market uncertainty during COVID-19, generating significant profits. However, it fails to recognize the market impact of the Russian invasion and the collapse of the Silicon Valley Bank. The Sharpe ratio of the strategy is 0.19 given the high standard deviation of it. For this reason it does not seem really appealing.

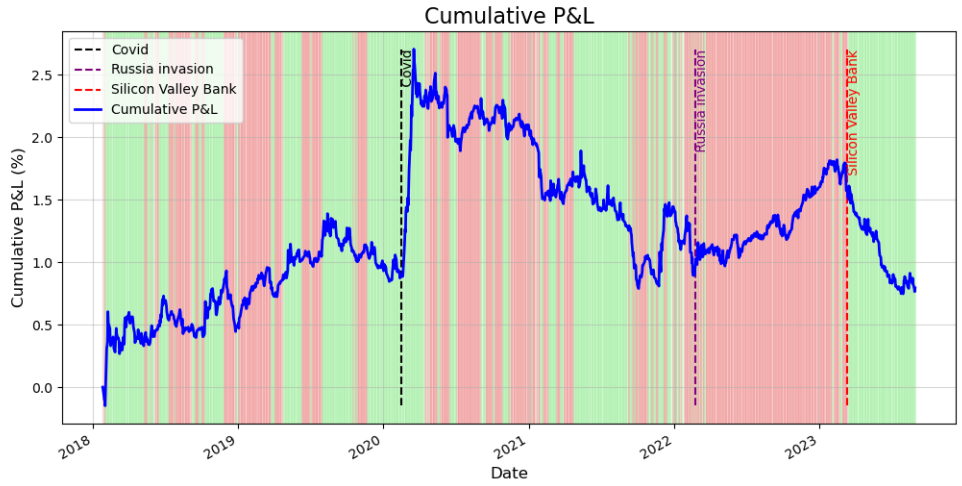

Figure 6: Cumulative P&L Long-Short Strategy
Cumulative P&L of the "buy rough, sell smooth" strategy for *VXX*, with green (long) and red (short) regions indicating open trading positions. The strategy captures COVID-19 volatility but does not capture other events, yielding a Sharpe ratio of 0.19.

5.1 Selling volatility

Selling volatility is often profitable until a sudden market event leads to substantial losses. For instance, a short volatility strategy during the COVID-19 period could have resulted in catastrophic drawdowns. To address this inherent risk, we aim to test whether our roughness parameter H can serve as a predictive signal to identify periods of extreme volatility and act as a "stop-trading" mechanism for a short volatility strategy.

Specifically, we backtest a simplified version of the original strategy, restricting it to short positions only, and evaluate whether H estimates can effectively mitigate risk during volatile market conditions. The results of this backtest are displayed in Figure (7):

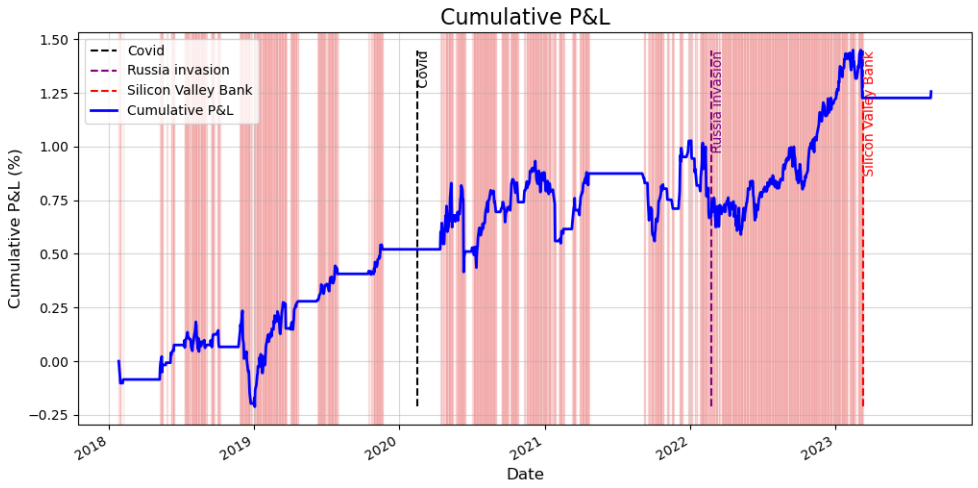

Figure 7: Cumulative P&L Short Strategy
Cumulative P&L of the "short volatility" strategy for *VXX*, red (short) regions indicating open trading positions. The strategy stops during COVID-19, but still yields a Sharpe ratio of 0.54.

The strategy demonstrates solid profitability, achieving a Sharpe Ratio of 0.54, with significantly reduced drawdowns compared to the original approach. A key advantage is that the roughness parameter H effectively identifies periods of extreme market uncertainty, serving as a valuable risk management tool. Notably, the strategy ceases trading during the onset of the COVID-19 crisis (starting in late 2019). Similarly, it halted trading during the collapse of Silicon Valley Bank, highlighting its ability to mitigate risks in turbulent market conditions.

6 Conclusion

In this project, we have examined the rough Bergomi framework for modeling volatility and its application to the VIX futures market. By calibrating the rBergomi model to a comprehensive dataset of VIX futures, we confirmed that the roughness parameter H consistently resides below the 0.5 threshold, in line with the rough volatility literature. Our empirical results indicate that H exhibits interesting time-series properties around market turbulence.

Although we tested a *simple buy rough, sell smooth* strategy based on the relative level of H, its performance was mixed, capturing certain market dislocations (e.g., during COVID-19) but missing others. A purely *short-volatility* approach enhanced with an H-driven stop-trading mechanism proved more robust, producing a more favorable Sharpe ratio and avoiding the most significant drawdowns. This outcome highlights one practical benefit of monitoring H: it can potentially serve as a tool to sidestep catastrophic losses during volatility spikes.

Overall, our findings underscore the significance of rough volatility modeling for both theoretical understanding and practical decision-making. While we demonstrated one possible way to use H for trading, further refinements could include more sophisticated signal filters, risk metrics, or multi-asset generalizations. In addition, future research might investigate whether additional market variables or enhance its use in real-time risk management.

References

C. Bayer, P. Friz, and J. Gatheral. Pricing uner rough volatility. *Quantitative Finance*, 16(6):1–18, 2015.

M. Bennedsen, A. Lunde, and M. Pakkanen. Decoupling the short- and long-term behavior of stochastic volatility. *Available at SSRN*, 2016. URL http://dx.doi.org/10.2139/ssrn.2846756.

L. Bergomi. Smile dynamics ii. *Risk*, pages 67–73, 2005. URL https://dx.doi.org/10.2139/ssrn.1493302.

P. Carr and D. Madran. Towards a theory of volatility trading. *Risk Publications*, pages 417–427, 1998.

D. Dufresne. The log-normal approximation in financial and other computations. *Advanced Applied Probability*, 36:747–773, 2004.

O. El Euch and M. Rosenbaum. The characteristic function of rough heston models. *Mathematical Finance*, 29(1):3–38, 2019. doi: https://doi.org/10.1111/mafi.12173. URL https://onlinelibrary.wiley.com/doi/abs/10.1111/mafi.12173.

J. Gatheral and A. Jacquier. Arbitrage-free svi volatility surfaces. *Quantitative Finance*, 14(1):59–71, 03 2014. URL http://dx.doi.org/10.2139/ssrn.2033323.

J. Gatheral, T. Jaisson, and M. Rosenbaum. Volatility is rough. *Quantitative Finance*, 18(6):933–949, 2018. doi: 10.1080/14697688.2017.1353127. URL https://dx.doi.org/10.2139/ssrn.2509457.

P. Glasserman and P. He. Buy rough, sell smooth. *Quantitative Finance*, 12 2020. URL http://dx.doi.org/10.2139/ssrn.3301669.

S. L. Heston. A closed-form solution for options with stochastic volatility with applications to bond and currency options. *The Review of Financial Studies*, 6(2):327–343, 04 2015. ISSN 0893-9454. doi: 10.1093/rfs/6.2.327. URL https://doi.org/10.1093/rfs/6.2.327.

A. Jacquier, C. Martini, and A. Muguruza. On vix futures in the rough bergomi model. *Quantitative Finance*, 18 (1):45–61, 2018. doi: 10.1080/14697688.2017.1353127. URL https://doi.org/10.1080/14697688.2017.1353127.